Biophysical Chemistry 40 (1991) 329–337
Elsevier Science Publishers B.V., Amsterdam

BIOCHE 01581

A ^{35}Cl and ^{37}Cl NMR study of chloride binding to the erythrocyte anion transport protein

William S. Price [a], Philip W. Kuchel [a,*] and Bruce A. Cornell [b]

[a] *Department of Biochemistry, University of Sydney, Sydney, NSW 2006 (Australia)*
[b] *CSIRO Division of Food Processing, North Ryde, NSW 2113 (Australia)*

Received 7 May 1990
Revised manuscript received 30 January 1991
Accepted 5 February 1991

NMR, $^{35}Cl^-$, $^{37}Cl^-$; Anion transport protein (band 3); Binding; Chloride ion; Erythrocyte (human); Quadrupolar relaxation

Band 3, the erythrocyte anion transport protein, mediates the one-for-one exchange of bicarbonate and chloride ions across the membrane and consequently plays an important role in respiration. Binding to the protein forms the first step in the translocation of the chloride across the membrane. ^{35}Cl and ^{37}Cl NMR relaxation measurements at various field strengths were used to study chloride binding to the protein in the presence and absence of the transport inhibitor 4,4′-dinitrostilbene-2,2′-disulfonate. Significant differences occurred in the NMR relaxation rates depending on whether the inhibitor was present or not. The results indicate that the rate of chloride association and dissociation at each external binding site occurs on a time scale of ≤ 5 μs. This implies that the transmembrane flux is not limited by the rate of chloride binding to the external chloride binding site of band 3. The rotational correlation-time of chloride bound to band 3 was found to be > 20 ns with a quadrupole coupling constant of ~ 3 MHz.

1. Introduction

The transport of Cl^- across the erythrocyte membrane plays an important role in the removal of CO_2 from the body [1]. The integral membrane protein, band 3, exchanges HCO_3^- and Cl^- in a one-to-one ratio. Band 3 is also able to transport other inorganic and organic anions and dicarboxylic acids [2]. It has also been suggested that band 3 is the route of water transport but later evidence has cast doubt on this suggestion [3]. Band 3 is a 95-kDa single polypeptide chain, and is the most abundant transport protein in the red cell [1,2]. Immunologically related proteins have been found in other plasma membranes, including the Golgi membranes [4]. Presently, the best model of the anion exchange process is that of a "ping-pong" carrier [5]. The process has been found to be both pH and charge dependent, thus band 3 is termed a "titratable anion carrier" [6,7].

We report here results of ^{35}Cl and ^{37}Cl NMR relaxation studies of Cl^- binding to the band 3 transport sites and its modification by the anion transport inhibitor 4,4′-dinitrostilbene-2,2′-disulfonate (DNDS; [8]). This inhibitor binds exclusively to the outward-facing transport site of the band 3 molecule [9] in the ratio of one DNDS molecule per band 3 monomer. It possesses a negative charge on the sulfonate and is capable of fully occupying the anion transport site of the protein; however, only the *trans*-isomer is inhibitory [10]. The DNDS binding site on band 3 is in a hydrophobic region within the bilayer, which restricts free rotation of the DNDS molecule [1].

The NMR technique used to study the binding of Cl^- is based on the large difference in relaxation rate between the free and bound species

* To whom correspondence should be addressed.

0301-4622/91/$03.50

[11,12]. The resonance corresponding to the bound species is generally invisible due to the rapid relaxation; however, if exchange between the free and the bound form is sufficiently rapid, the resonance from the free species will be broadened. The broadened spectral line will then contain information on the rate of exchange between the two sites and the binding site itself [12]. Previous ^{35}Cl and ^{37}Cl NMR binding studies of band 3 [9,13–16] have relied on measuring the effect of binding by its resultant increase in linebroadening. However, in the experiments reported here, actual relaxation times were measured directly using multipulse techniques which are more reliable than linebroadening analysis and they are not susceptible to 'instrumental (inhomogeneous field)' broadening [17].

2. Materials and methods

2.1 Reagents

Tris–HCl was obtained from Sigma. 4,4′-Dinitrostilbene-2,2′-disulfonate was from Pfaltz & Bauer. Deuterated H_2O was obtained from the Australian Institute of Nuclear Science and Engineering, Lucas Heights, NSW, Australia. All other reagents were of A.R. grade. Human blood was obtained from the Red Cross Blood Transfusion Service, Sydney, NSW, Australia within 48 hours from being taken by venipuncture.

2.2 Preparation of 'leaky' erythrocyte ghosts

Red cells were washed three times in saline (154 m*M* NaCl; 277 K). The cells were then lysed in ~15 volumes of hemolysis buffer (15 m*M* Tris–HCl; 1 m*M* EDTA; pH 7.4; 277 K). The EDTA was included in the buffer to chelate any paramagnetic ions present. The hemolysate was then recycled through a hollow fibre system [18] with fresh hemolysis buffer until the erythrocyte ghosts appeared hemoglobin free (~3 hours). The ghosts were then pelleted by centrifugation at 34,800 *g* for 20 min. Then the ghosts were washed three times in "NMR buffer" (50:50 saline:hemolysis buffer, giving a Cl^- concentration of 84.5 m*M*) by centrifugation at 34,800 *g* for 20 min. Finally the ghosts were resuspended in NMR buffer and centrifuged at 110,000 *g* for 30 min to pellet the membranes. The entire membrane preparation was conducted at 277 K.

2.3 NMR sample preparation

Membrane samples with, and without DNDS, were prepared by taking two aliquots of the membrane preparation; to one was added DNDS (201 m*M* DNDS in NMR buffer) to a final concentration of 1 m*M* and the same volume of neat NMR buffer was added to the other sample. This protocol ensured that both samples had identical membrane concentrations. Buffer samples with, and without, DNDS were prepared similarly.

Volumes of 3 ml of the samples were dispensed into 10 mm o.d. NMR tubes except for samples used with the Bruker CXP-300 spectrometer, in which case ~2 ml were placed into glass ampules and flame sealed.

2.4 NMR spectroscopy

^{35}Cl relaxation measurements were recorded at three different field strengths, corresponding to ^{35}Cl resonance frequencies of 8.8, 29.4 and 39.2 MHz. ^{37}Cl relaxation measurements were conducted at 32.6 MHz. Three spectrometers were used in performing these measurements: Varian XL/VXR 400, Bruker CXP-300 and CXP-100. Typically, measurements performed on the CXP-100 and CXP-300 spectrometers employed a spectral width of 5000 Hz digitized into 4 K data points with a $\pi/2$ pulse length of 16 μs. Measurements performed on the XL/VXR 400 spectrometer generally used a spectral width of 2500 Hz digitized into 4 K data points with a $\pi/2$ pulse length of 74 μs. Measurements at all four resonance frequencies were conducted at 288 K. In addition, measurements of ^{37}Cl and ^{35}Cl relaxation at 32.6 and 39.2 MHz, respectively, were conducted at 293 K. The T_1 measurements were performed using the inversion-recovery pulse sequence [19]. T_2 measurements were made using the Hahn spin-echo pulse sequence [20,21]. $T_{1\rho}$ measurements [22] were only conducted at 8.8 and

29.4 MHz due to instrumental limitations; a delay of 4 s was allowed between each transient to minimize sample heating.

2.5 Numerical analysis

Non-linear least squares analyses was performed using the modified Levenberg–Marquardt–Morrison algorithm [23] to regress the appropriate two or three parameter functions onto the relaxation data. Where relaxation measurements were repeated the weighted arithmetic mean and (grouped) standard deviation [24] were used.

2.6 Protein assays

Total protein in erythrocyte ghosts was assayed using the Lowry method [25] modified by the addition of sodium dodecyl sulfate [26].

3. Theory

3.1 Relaxation theory

For nuclei with spin quantum number $I > 1/2$ the dominant relaxation mechanism, providing there are no paramagnetic species present, is due to the coupling of the nuclear quadrupole moment, Q, to an electric field gradient, eq, generated by a non-cubic distribution of charge about the nucleus. Fluctuations in the field gradient cause modulation of nuclear energy and hence relaxation of the high energy nuclear state [27,28]. It has been found that the relevant fluctuations are those resulting from the electric field gradients in the first coordination sphere of the chloride ion. Thus the relaxation of the chloride ions reflects interactions with its nearest neighbours [29].

Because ^{35}Cl and ^{37}Cl both have $I = 3/2$, the time dependence of the longitudinal and transverse magnetization, M_z and $M_{x,y}$, respectively, are both described by a sum of two exponentials: the general expressions for these relaxations are [30];

$$M_z(t) - M_{ze} = \left(M_z(0) - M_{ze}\right)\left\{0.2\exp\left(-t/T_1^{\mathrm{f}}\right) + 0.8\exp\left(-t/T_1^{\mathrm{s}}\right)\right\}, \quad (1)$$

$$M_{x,y}(t) = M_{x,y}(0)\left\{0.6\exp\left(-t/T_2^{\mathrm{f}}\right) + 0.4\exp\left(-t/T_2^{\mathrm{s}}\right)\right\}, \quad (2)$$

where the superscripts 'f' and 's' denote fast and slow, respectively, and the subscript 'e' denotes equilibrium magnetization. The various relaxation times are defined in the next section. Equation (2) can be modified to express relaxation in the rotating frame ($T_{1\rho}$) by making the appropriate substitution for T_2^{f}.

3.2 Relaxation and exchange

In the presence of binding, the nuclear populations in different sites normally have the same chemical shift but are characterized by different relaxation times [28]. Binding may be defined as the residence of the ion at a given site for a period "several orders of magnitude greater than the correlation-time" [31]. Considerable simplicity is introduced into the analysis of the relaxation data by the fact that each of the two components of T_1 and T_2 relaxation, for nuclei with $I = 3/2$, behave as if they exchange independently with the corresponding component from other fractions [32]. For the case of 'intermediate' rates of exchange between free Cl^- ions and small populations of bound ions (P_i) with relaxation time $T_{x\mathrm{B}}^{y}$ ($x = 1, 2, 1\rho$; $y =$ f or s, the subscript 'B' denotes the bound state), and exchange lifetimes τ_{ex}, the magnetization decays are given by [32–34];

$$1/T_1^{\mathrm{f}} = 1/T_{1\mathrm{free}} + \sum_i \left[P_i/\left(T_{1\mathrm{B}}^{\mathrm{f}} + \tau_{\mathrm{ex}}\right)\right], \quad (3)$$

with similar expressions for T_1^{s}, T_2^{f}, T_2^{s}, $T_{1\rho}^{\mathrm{f}}$. The subscript 'free' denotes the free Cl^-. The relaxation rate constants of the bound Cl^- are (assuming that isotropic motions dominate the relaxation pathway of the bound Cl^-):

$$1/T_{1\mathrm{B}}^{\mathrm{f}} = 0.4\pi^2\chi^2 J(\omega_0), \quad (4)$$

$$1/T_{1\mathrm{B}}^{\mathrm{s}} = 0.4\pi^2\chi^2 J(2\omega_0), \quad (5)$$

$$1/T_{2\mathrm{B}}^{\mathrm{f}} = 0.2\pi^2\chi^2\left[J(0) + J(\omega_0)\right], \quad (6)$$

$$1/T_{2\mathrm{B}}^{\mathrm{s}} = 1/T_{1\rho\mathrm{B}}^{\mathrm{s}} = 0.2\pi^2\chi^2\left[J(\omega_0) + J(2\omega_0)\right], \quad (7)$$

$$1/T_{1\rho B}^{f} = 0.2\pi^2\chi^2\left[J(2\omega_1) + J(\omega_0)\right], \quad (8)$$

$$J(\omega) = \tau_c/\left(1 + \omega^2\tau_c^2\right), \quad (9)$$

where $\chi = e^2qQ/h$ is the quadrupolar coupling constant (in Hz), ω_0 is the precession frequency in the main field, ω_1 is the nuclear magnetic precession frequency in the rotating frame, τ_c is the correlation time of the relaxing species and the $J(x)$ ($x = 0$, ω_0, ω_1) are spectral density functions.

Often the magnetization decay appears to be single exponential [32], in which case the following approximations can be used for the "apparent" single exponential time constants [32].

$$1/T_1 = 1/T_{1free} + \sum_i P_i\left\{0.8/\left(T_{1B}^{s} + \tau_{ex}\right) + 0.2/\left(T_{1B}^{f} + \tau_{ex}\right)\right\}, \quad (10)$$

$$1/T_2 = 1/T_{2free} + \sum_i P_i\left\{0.4/\left(T_{2B}^{s} + \tau_{ex}\right) + 0.6/\left(T_{2B}^{f} + \tau_{ex}\right)\right\}, \quad (11)$$

$$1/T_{1\rho} = 1/T_{1\rho free} + \sum_i P_i\left\{0.4/\left(T_{1\rho B}^{s} + \tau_{ex}\right) + 0.6/\left(T_{1\rho B}^{f} + \tau_{ex}\right)\right\}, \quad (12)$$

4. Results

All samples contained a protein concentration of ~6.5 mg/ml. If it is assumed that band 3 constitutes 25% of all protein present in the erythrocyte membrane [35], then the band 3 concentration in the NMR samples was 17 μM. At 273 K the outside ($K_{o,1/2max}$) and inside ($K_{i,1/2max}$) chloride ion concentrations, which cause a half maximal flux when the concentration on the opposite side of the membrane saturates the transport system are 3.9 and 61.1 mM, respectively [36]. In the present study the chloride concentration was 84.5 mM and so it is reasonably assumed that all the outward facing band 3 sites are oc-

Table 1

Single exponential analysis of relaxation of magnetization to give values for T_1, $T_{1\rho}$ and T_2 of $^{35}Cl^-$ and $^{37}Cl^-$ in membrane suspensions (with, and without DNDS) and buffer [a]

Temp (K)	Freq (MHz)	T_1 (ms)			T_2 (ms)			$T_{1\rho}$ (ms)		
		Membranes		Buffer	Membranes		Buffer	Membranes		Buffer
		−DNDS	+DNDS		−DNDS	+DNDS		−DNDS	+DNDS	
288	8.819	13.4±0.4	16.6±0.3	27.3±0.2	6.3±0.8	8.5±0.5	25.1±0.7	5.0±0.3	8.1±0.7	25.5±0.8
	29.400	21.5±0.2	22.4±0.2	32.9±0.5	9.6±0.6	12.2±0.5	32.7±1.2	5.2±0.3	7.2±0.5	34.1±0.8
	32.648	31.7±0.7	33.7±0.8	47.7±0.9	17.2±1.2	22.4±0.7	47.0±1.8			
	39.187	20.2±0.2	21.8±0.2	29.7±0.1	12.4±0.6	14.8±0.3	30.2±0.3			
293	32.648	36.3±0.6	39.7±0.7	54.3±0.6	16.2±0.9	25.2±1.1	50.9±1.1			
	39.187	24.1±0.2	25.8±0.1	32.2±0.1	12.7±0.6	16.7±0.5	32.6±0.2			

[a] Relaxation times are not given for the Cl^- ions in DNDS-containing buffer since they were, within experimental error, the same as those of the buffer samples that did not contain DNDS. Relaxation times are for $^{35}Cl^-$ except for the measurements performed at 32.6 MHz which are for $^{37}Cl^-$ in a field of 9.4 T. $T_{1\rho}$ measurements were not made at 32.6 or 39.2 MHz due to limitations of the spectrometer. T_1 values were computed using the equation:

signal amplitude $= -A + (A + H)\exp(-t/T_1)$,

where A and H are constants. $T_{1\rho}$ and T_2 values were computed by regressing either a two (A) or three (B) parameter function onto the data, viz:

signal amplitude $= H\exp(-t/T_x)$ (A)

signal amplitude $= H\exp(-t/T_x) + A$ (B)

where $T_x = T_{1\rho}$, T_1 or $T_2/2$ (since a Hahn spin-echo pulse sequence was used to measure T_2). The choice of a 2 or 3 parameter function depended on whether realistic values were obtained for the baseline correction constant (A).

Table 2

Double exponential analysis of relaxation of magnetization [a]. The fast and slow components of T_2 and $T_{1\rho}$ relaxation of ^{35}Cl and ^{37}Cl in the membranes without, and the membranes with DNDS.

Temp (K)	Freq (MHz)	Membranes							
		−DNDS		+DNDS		−DNDS		+DNDS	
		T_2^f (ms)	T_2^s (ms)	T_2^f (ms)	T_2^s (ms)	$T_{1\rho}^f$ (ms)	$T_{1\rho}^s$ (ms)	$T_{1\rho}^f$ (ms)	$T_{1\rho}^s$ (ms)
288	8.819	4.5±0.9	11.3±1.2	6.1±0.5	19.4±1.3	3.8±0.3	11.4±1.1	6.6±0.6	25.1±0.3
	29.400	4.6±0.2	19.2±0.2	7.7±0.4	21.5±0.7	3.7±0.1	14.8±0.7	5.5±0.3	25.6±1.8
	32.648	9.3±1.4	40.7±3.2	15.0±1.2	39.0±2.5				
	39.187	6.5±0.4	24.2±0.6	10.2±0.4	23.7±0.6				
293	32.648	8.7±0.7	47.5±2.5	16.9±1.0	53.1±3.1				
	39.187	7.2±0.3	28.8±0.9	11.5±0.3	31.3±0.7				

[a] The values at 32.6 MHz were for ^{37}Cl in a magnetic field of 9.4 T. $T_{1\rho}$ measurements were not determined at 32.6 and 39.2 MHz. The values were computed using the equations:

$$\text{signal amplitude} = H\left\{0.6\exp\left(-t/T_2^f\right)+0.4\exp\left(-t/T_2^s\right)\right\},$$

$$\text{signal amplitude} = H\left\{0.6\exp\left(-t/T_{1\rho}^f\right)+0.4\exp\left(-t/T_2^s\right)\right\}.$$

cupied by a Cl ion (thus preventing binding to the inward facing sites). Thus the fraction of chloride ions bound is $\sim 2.0\times10^{-4}$ of the total, leaving the bulk of the Cl^- present in free solution.

The $^{35}Cl^-$ and $^{37}Cl^-$ NMR relaxation times obtained using single exponential analysis measured in buffer and in the presence of the membranes are shown in Table 1. The T_1 and T_2 values were the same within experimental error, at all frequencies for the buffer samples, but differed for membrane samples. The difference between T_1 and T_2 values for the membrane-containing samples indicated that the extreme narrowing limit (at which $\omega\tau_c \ll 1$) was not attained at the Cl^- binding site [37], thus justifying the choice of the relaxation model embodied in eqs. (1)–(12). From the theory presented above, it can be seen that when $\omega\tau_c > 1$ the two components of T_2 (namely T_2^f and T_2^s) and $T_{1\rho}^f$ (namely $T_{1\rho}^f$ and $T_{1\rho}^s$) should be significantly different and hence may possibly be determinable by regression analysis of relaxation time-courses. Such is not the case for longitudinal relaxation since the contributions to the rate of relaxation of $1/T_{1B}^f$ and $1/T_{1B}^s$ differ by less than a factor of four. Hence, only T_2 and $T_{1\rho}$ data were able to be analysed into two exponentially relaxing components: the results are given in Table 2. However, the errors resulting from a double exponential analysis are often large [32,34].

The *difference* between relaxation rate constants (called the 'excess' relaxation rate constant) for Cl ions in the membrane samples with, and

Table 3

Excess relaxation rate constants (i.e., the *difference* between the relaxation rate constants for the membrane without and membrane with DNDS) calculated from the data in Table 1. The values at 32.6 MHz are for ^{37}Cl. $T_{1\rho}$ measurements were not measured (nm) at 32.6 or 39.2 MHz

Temp (K)	Freq (MHz)	$\Delta 1/T_1$ (s^{-1})	$\Delta 1/T_2$ (s^{-1})	$\Delta 1/T_{1\rho}$ (s^{-1})	$\Delta 1/T_2^f$ (s^{-1})	$\Delta 1/T_2^s$ (s^{-1})	$\Delta 1/T_{1\rho}^f$ (s^{-1})	$\Delta 1/T_{1\rho}^s$ (s^{-1})
288	8.819	14.4±3.3	41±27	77±23	58±58	37 ±13	111±35	48±9
	29.400	1.9±0.8	22±10	53±21	88±16	5.6± 2.1	88±17	29±6
	32.648	1.9±1.4	14± 5	nm	41±22	−1.1± 3.6	nm	nm
	39.187	3.6±0.9	13± 5	nm	56±13	−0.9± 2.1	nm	nm
293	32.648	2.4±0.9	22± 5	nm	56±13	2.2± 2.2	nm	nm
	39.187	2.7±0.5	19± 6	nm	52± 8	2.8± 1.8	nm	nm

without, DNDS, was used to study the chloride binding. The excess longitudinal and transverse relaxation rate constants are denoted by $\Delta(1/T_1)$ and $\Delta(1/T_2)$, respectively. The excess relaxation rate constants "report" on Cl^- binding to band 3 and the particular values are given in Table 3.

From the measured excess relaxation rate constants numerical simulations were used to determine values for τ_{ex}, τ_c, and the quadrupole coupling constant of the Cl^- bound to band 3. Values for τ_{ex}, τ_c, and the quadrupole coupling constant were inserted into eqs. (1)–(12) and the values were adjusted in order to simulate the experimentally determined values. The quadrupole moments used in the calculations were -0.082×10^{-28} and -0.065×10^{-28} m^2 for ^{35}Cl and ^{37}Cl, respectively [38]. An initial estimate of the correlation-time of the Cl ion bound to band 3 was

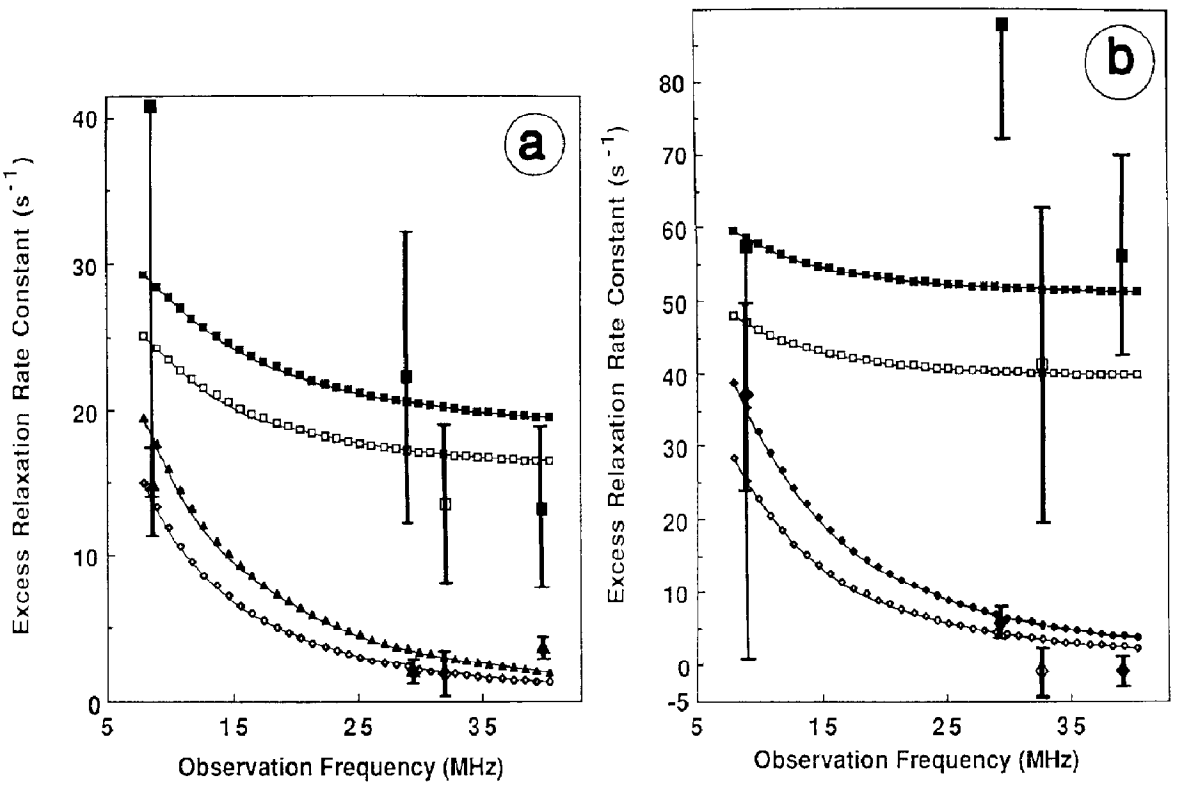

Fig. 1. Numerical simulations (evaluations) of the expressions given by eqs. (1)–(12) for the excess relaxation rate constants for Cl^- binding to band 3. The aim was to simulate the observed excess relaxation rate constants for Cl^- at the band 3 binding site (see Table 3) given values for τ_{ex}, τ_c, and the ^{35}Cl quadrupole coupling constant (χ). The ^{37}Cl quadrupole coupling constant was obtained by multiplying χ by the ratio of the quadrupole moments of the two chlorine isotopes. The values of τ_c and χ refer to Cl^- bound to band 3. The fraction of the Cl^- population bound was set to 2.01×10^{-4} (see text). It should be kept in mind when comparing the simulated excess relaxation data with the experimental values that the experimental values have inherently large errors, as indicated. The large errors result because the excess relaxation rate constant is calculated by substrating the inverses of two small numbers which already contain an appreciable error (see Tables 1 and 2). This is especially true for the 8.8 MHz data. (a) The excess relaxation rate constants versus NMR observation frequency for ^{35}Cl derived from T_1 (△) and T_2 (■) simulations and for ^{37}Cl derived from T_1 (◇) and T_2 (□) simulations, both with assuming analysis using a single exponential expression. The parameter values used in eqs. (10)–(12) were $\tau_c = 25$ ns, $\tau_{ex} = 4.8 \times 10^{-6}$ s and Q 3.3 MHz. The corresponding experimental data obtained at 288 K from Table 3, are plotted with the corresponding larger symbols and with error bars. (b) The excess relaxation rate constants versus NMR observation frequency for ^{35}Cl derived from T_2^f (■) and T_2^s (◆) simulations and for ^{37}Cl derived from T_2^f (□) and T_2^s (◇) simulations, both with analysis using a double exponential expression. The parameter values used in eqs. (4)–(9) were $\tau_c = 22$ ns, $\tau_{ex} = 2.0 \times 10^{-6}$ s and $Q = 3.4$ MHz. The corresponding experimental data obtained at 288 K, from Table 3, are plotted with the corresponding larger symbols and with error bars.

obtained by examining the frequency dependence of the excess relaxation rate constants at the band 3 site (i.e., DNDS-sensitive site; Table 3). From the data it appears that $\omega\tau_c \approx 1$ at $\omega/(2\pi) < 8.8$ MHz thus implying that $\tau_c > 18$ ns. Example simulations are shown in Fig. 1. The three parameter values which best fitted the values of the single exponentially derived excess relaxation rate constants were $\tau_{ex} \sim 4.8 \times 10^{-6}$ s, $\tau_c \sim 25$ ns, and a ^{35}Cl quadrupole coupling constant ~ 3.3 MHz. From simulations of the double exponentially derived excess relaxation rate constants the corresponding best set of values was $\sim 2.0 \times 10^{-6}$ s, ~ 22 ns and ~ 3.4 MHz. Because the $T_{1\rho}$ measurements were conducted at only two field strengths, their excess relaxation rate constants were not considered in the simulations.

5. Discussion

Estimates of relaxation times obtained from measurements of linewidth are more susceptible to instrumental artifacts than those obtained by multipulse methods [39]. This is especially true for nuclei with $I = 3/2$, since the slowly relaxing components are more heavily weighted in the line-shape analysis. The T_2 values were measured using a Hahn spin-echo sequence instead of the more generally used Carr–Purcell–Meiboom–Gill sequence [40] in order to minimize sample heating (e.g., [41]). The relaxation measurements were, when duplicates were conducted, generally reproducible (i.e., within experimental error). Translational diffusion of the Cl ions made a negligible contribution to the measured T_2 values as is evident from the close agreement with the T_1 values for the buffer sample.

Due to different experimental conditions only an approximate comparison is able to be performed between the ^{35}Cl relaxation measurements conducted at 8.8 MHz and 288 K in the present work and the line-shape analysis of Falke et al. [14]. The comparison is made as follows: from Fig. 3 of Falke et al. [14], the excess transverse relaxation rate constant can be calculated to be 48.8 s^{-1} (6.5 mg/ml protein) at 276 K, our experimental value, at 288 K, is 41.1 s^{-1} (see Table 3). By substituting our values, derived from single exponential analysis for τ_c, τ_{ex}, and χ, and allowing for the chloride concentration used by Falke et al., [14] (three times that in the present work) into eq. (11) the transverse excess relaxation rate constant was calculated to be 9.6 s^{-1}: using the present chloride concentration a value of 28.6 s^{-1} was obtained.

Although the relaxation of bound Cl^- is multiexponential, because the bound Cl^- motion is not in the extreme narrowing limit, single exponential analysis was used as well as double exponential analysis to compute the relaxation rate constants. There were two reasons for this: First, pronounced deviations from single exponential decay for Cl^- and other $I = 3/2$ nuclei are usually not observed and have generally only been seen with $^{23}Na^+$; second, it has been shown, using a perturbation treatment, that quadrupole relaxation in the presence of chemical exchange is well described by a single exponential decay, provided that the values of the spectral density functions are only weakly frequency-dependent [39]. Double exponential analysis is theoretically correct, but the analysis of the relaxation time courses is less likely to give a unique estimate of parameter values. Conversely, single exponential analysis is simpler but the equations relating the relaxation time constants to the binding parameters are only approximations [32]. With both single and double exponential analysis the T_2 measurements were found to be more sensitive to Cl^- binding than the T_1 measurements (see Tables 1 and 3).

A model involving relaxation by anisotropic motion [42] may be more appropriate for analysing our data than the isotropic model. However, the anisotropic model involves considerable computational difficulties because the T_1 and T_2 relaxation times of Cl^- in membrane suspensions in the presence or absence of DNDS, were only marginally different; only if they were very different would fitting of the more complicated model, with its additional parameters, be possible.

In a red cell membrane about 40% of band 3 is anchored to the cytoskeleton, hindering its rotational diffusion [43]. In the present study the membranes were isolated using buffers containing

EDTA which at higher concentrations can be used to extract the cytoskeleton protein, spectrin, from the membranes. However, due to the low temperature at which the preparation was performed, together with the low EDTA concentration used (i.e., 1 m*M*), spectrin removal would have been minimal (G. Ralston, personal communication). Also, to our knowledge, no relationship has been shown between band 3 rotational diffusion and ion transport. Hence it is unlikely that the present binding phenomena were influenced by cytoskeletal changes.

Falke et al. [9] claimed that their "crushed ghosts", suspended in 250 m*M* Cl^-, remained crushed to such an extent that the internal Cl^- ions were in slow exchange with the external solution and thus no longer contributed to the observed linebroadening. However, in our procedure the ghosts were first prepared by a more gentle technique and then pelleted from 84.5 m*M* Cl^- at 110,000 *g*. The negative charges of the phosphatidylserine headgroups on the inner face of the membranes [44] repel each other at low salt concentrations, keeping the bilayers separated (G. Ralston, personal communication). Also the measurements presented in this paper were performed at temperatures at least 12 K higher than those of Falke and co-workers which would increase the rate of exchange due to the greater diffusion coefficient of the Cl^- ions. Hence we assume that the holes in the membranes caused by osmotic lysis [45,46] allow rapid exchange, on the NMR time scale, of chloride ions between the internal and external compartments. Thus the relaxation effects measured in this study could result from both internal and external binding sites. In addition it was assumed that Cl^- ions move between two binding sites via the free solution. However, because of the asymmetry of the Cl^- binding constants between the inward and outward facing band 3 sites (*vide supra*), the results of the present study will relate predominantly to Cl^- binding to the outward facing sites. When Cl ions bind to band 3, translocation can occur as well as dissociation, but the dissociation rate is very rapid compared to the translocation rate (translocation rate constant 400 s^{-1} at 273 K [10]).

The non-DNDS specific NMR relaxation of Cl^- in the membrane-containing samples is unlikely to result from viscosity effects on the correlation-time of the ion. The macroscopic viscosity is largely determined by the membranes, and the motion of the much smaller Cl^- ions should be virtually unaffected [47]. For example, the nonconformity of bulk viscosity and the viscosity probed by NMR measurements has been exhibited with a small phosphorus-containing molecule [48]. Thus it appears that the non-DNDS specific relaxation must largely result from the presence of at least one other type of binding site on the leaky ghost membranes; this is consistent with the findings of Falke and coworkers [14]. Analysis using the excess relaxation rates for non-DNDS specific relaxation in the membrane samples was not included since it seemed unjustified to assume that the sites would form a homogeneous population.

Under optimal conditions the temperature dependence of the excess relaxation rate constants (see Table 3) or the ratio of the excess relaxation rate constants of ^{35}Cl to ^{37}Cl can be used to infer "the time scale of the exchange process" [11]. However, in the present study these methods did not clearly define the time scale.

Single and double exponential analysis gave suprisingly similar results with the largest discrepancy being in the estimates of the exchange lifetime, τ_{ex}. The values obtained for the rotational correlation-time of Cl^- bound to band 3 are similar to values observed for Cl^- binding to alcohol dehydrogenase [49]. Falke and Chan [13] proposed that an arginine may be involved in the binding of Cl to band 3. Bull et al., [49] have estimated the quadrupole coupling constant for Cl^- bound to the $C(NH_2)^+$ group of an arginine to be 2.8 MHz. This value is in reasonable agreement with the value determined in the present work. The exchange time determined here, implies that the rates of chloride association and dissociation at the outward facing band 3 sites occur on a time scale of ≤ 5 μs. The value obtained for the exchange time is similar to that obtained by Falke et al., [15] and hence the association/dissociation of chloride onto the outward facing band 3 binding site should not limit the transmembrane chloride flux.

Acknowledgements

The work was supported by a grant to PWK from the Australian NH&MRC. WSP received a Commonwealth Postgraduate Research Award. Dr. R.J. Pace is thanked for discussions on the binding experiments and Mr. W.G. Lowe for technical assistance. Dr. W.A. Bubb and Mr. F. Crino are thanked for assistance with the NMR work and Mr. B.T. Bulliman for assistance with computing.

References

1 I.G. Macara and L.C. Cantley, Cell Membr. 1 (1983) 41.
2 P.A. Knauf, Curr. Top. Membr. Transp. 257 (1979) 249.
3 J. Fischbarg, L.S. Liebovitch and J.P. Koniarek, Biochim. Biophys. Acta 898 (1987) 266.
4 S. Kellokumpu, L. Neff, S. Jämsä-Kellokumpu, R. Kopito and R. Baron, Science 242 (1988) 1308.
5 O. Fröhlich and R.B. Gunn, Biochim. Biophys. Acta 864 (1986) 169.
6 R.B. Gunn, in: Oxygen affinity of hemoglobin and red cell acid base status, eds. M. Rørth and P. Astrup (Munksgard, Copenhagen, 1982) p. 823.
7 R.B. Gunn, Membr. Transp. Proces., 1 (1978) 61.
8 J.J. Falke and S.I. Chan, Biochemistry 25 (1986) 7888.
9 J.J. Falke, R.J. Pace and S.I. Chan, J. Biol. Chem. 259 (1984) 6481.
10 O. Fröhlich and R.B. Gunn, Physiol. Sci., Proc. 28th, Int. Congr. 6 (1981) 275.
11 B. Lindman and S. Forsén, Chlorine, bromine and iodine NMR (Springer, Heidelberg, 1976).
12 S. Forsén and B. Lindman, Methods Biochem. Anal. 27 (1981) 289.
13 J.J. Falke and S.I. Chan, J. Biol. Chem. 260 (1985) 9537.
14 J.J. Falke, R.J. Pace and S.I. Chan, J. Biol. Chem. 259 (1984) 6472.
15 J.J. Falke, K.J. Kanes and S.I. Chan, J. Biol. Chem. 260 (1985) 9545.
16 J.J. Falke, K.J. Kanes and S.I. Chan, J. Biol. Chem. 260 (1985) 13294.
17 M. Holz and H. Weingärtner, J. Magn. Reson. 27 (1977) 153.
18 W.S. Price, B.D. Roufogalis and P.W. Kuchel, Anal. Biochem. 179 (1989) 190.
19 R.L. Vold, J.S. Waugh, M.P. Klein and D.E. Phelps, J. Chem. Phys. 48 (1968) 3831.
20 E.L. Hahn, Phys. Rev. 80 (1950) 580.
21 H.Y. Carr and E.M. Purcell, Phys. Rev. 94 (1954) 630.
22 M.L. Martin, G.J. Martin and J.J. Delpuech, Practical NMR spectroscopy, (Heyden, London, 1980) p. 255.
23 M.R. Osborne, J. Aust. Math. Soc. B. 19 (1976) 343.
24 M.R. Spiegel, Theory and problems of statistics, (McGraw-Hill, New York, NY, 1972).
25 O.H. Lowry, N.J. Rosebrough, A.L. Farr and R.J. Randall, J. Biol. Chem. 193 (1951) 266.
26 M.A. Markwell, S.M. Haas, L.L. Bieber and N.E. Tolbert, Anal. Biochem. 87 (1978) 206.
27 R.S. Stephens and R.G. Bryant, Mol. Cell. Biochem. 13 (1976) 101.
28 B. Lindman and S. Forsén, in: NMR and the periodic table, eds. R.K. Harris and B.E. Mann, (Academic Press, London, 1978) p. 421.
29 M. Yudasaka, T. Sugawara, H. Iwamura and T. Fujiyama, Bull. Chem. Soc. Jpn. 54 (1981) 1933.
30 P.S. Hubbard, J. Chem. Phys. 53 (1970) 985.
31 M.M. Civan and M. Shporer, in: Biological magnetic resonance, eds. L.J. Berliner and J. Reuben, vol 1, (Plenum Press, New York, NY, 1978) p. 1.
32 T.E. Bull, J. Magn. Reson. 8 (1972) 344.
33 B.A. Cornell, J.M. Pope and G.J.F. Troup, Chem. Phys. Lipids 13 (1974) 183.
34 H. Shinar and G. Navon, Biophys. Chem. 20 (1984) 275.
35 T.L. Steck, J. Cell Biol. 62 (1974) 1.
36 R.B. Gunn and O. Fröhlich, J. Gen. Physiol. 74 (1979) 351.
37 T.E. Bull, B. Lindman and P. Reimarsson, Arch. Biochem. Biophys. 176 (1976) 389.
38 J.W. Akitt, in: Multinuclear NMR, ed. J. Mason, (Plenum Press, New York, NY, 1987) p. 448.
39 B. Halle and H. Wennerström, J. Magn. Reson. 44 (1981) 89.
40 S. Meiboom and D. Gill, Rev. Sci. Instrum. 29 (1958) 688.
41 W.A. Bubb, K. Kirk and P.W. Kuchel, J. Magn. Reson. 77 (1988) 363.
42 D.E. Woessner, J. Chem. Phys. 36 (1962) 1.
43 V. Bennet, Ann. Rev. Biochem. 54 (1985) 273.
44 N.J. Russell, G.M. Powell, J.G. Jones, P.J. Winterburn and J.M. Basford, Blood biochemistry, (Croom Helm, London, 1982) p. 6.
45 M.R. Lieber and T.L. Steck, J. Biol. Chem. 257 (1982) 11651.
46 M.R. Lieber and T.L. Steck, J. Biol. Chem. 257 (1982) 11660.
47 J.-E. Norne, S.-G. Hjalmarsson, B. Lindman and M. Zeppezauer, Biochemistry 14 (1975) 3401.
48 W.S. Price, P.W. Kuchel and B.A. Cornell, Biophys. Chem. 33 (1989) 205.
49 T.E. Bull, B. Lindman, R. Einarsson and M. Zeppezauer, Biochim. Biophys. Acta 377 (1975) 1.